



Research Article

Complex Processing of Adsorbent Used in the Purification of Hydrogen-Containing Gas

Sukhrob Ibodullaev¹, Nurkhon Isaeva², Rustam Khodjiev³, Elena Mirzaeva⁴,
Dilnoza Turdieva², Shukhrat Gulomov², Shavkat Mamatkulov^{1,*}

¹*Institute of Material Science of the Uzbekistan Academy of Sciences, Ch. Aytmatov str.2B, Tashkent 100084, Uzbekistan.*

²*Center for Advanced Technologies, University str.7, Tashkent 100174, Uzbekistan.*

³*Bukhara Petroleum Refinery Plant Unitary Enterprise, Karaul-bazar, street Mustakillik 1, Bukhara Region 200900, Uzbekistan.*

⁴*Almalyk Branch of the National Research Technological University "MiSIS", Uzbekistan.*

Received: 27th September 2021; Revised: 29th October 2021; Accepted: 30th October 2021

Available online: 9th November 2021; Published regularly: March 2022



Abstract

The problems of processing spent adsorbents with a high concentration of chemisorbed chlorine-containing compounds for their reuse are studied in this article. The genesis of the phase composition and morphology at all technological stages of thermochemical regeneration of the spent adsorbent - Axstrap-860 by means of alkaline modification with a combined solution of sodium and potassium hydroxides has been tested by diffractometry and elemental analysis. The results show that the formation of a layer with an increased concentration of alkali metals in the form of the corresponding carbonates and NaOH on the surface of the granules and in the volume of sodium and potassium aluminates provides adsorption of HCl, which are slightly inferior to the fresh adsorbent. The conditions for the removal of halogen-containing substances from technogenic raw materials with the subsequent isolation of useful products have been optimized: (1) crystalline NaCl intended for the preparation of electrolyte for electrode boilers and steam generators; (2) a mixture of chlorides and hydroxochlorides of aluminum tested in the process of coagulation purification of turbid natural and waste waters; (3) pseudoboehmite for the production of an adsorbent-desiccant and the synthesis of magnesium-aluminum spinel using the technology of destruction-epitaxial transformation, and a promising carrier for catalysts for steam reforming of hydrocarbons.

Copyright © 2021 by Authors, Published by BCREC Group. This is an open access article under the CC BY-SA License (<https://creativecommons.org/licenses/by-sa/4.0>).

Keywords: Adsorbent; Catalyst carrier; Oil refining; Regeneration of catalysts; Hydrogen

How to Cite: S. Ibodullaev, N. Isaeva, R. Khodjiev, E. Mirzaeva, D. Turdieva, S. Gulomov, S. Mamatkulov (2022). Complex Processing of Adsorbent Used in the Purification of Hydrogen-Containing Gas. *Bulletin of Chemical Reaction Engineering & Catalysis*, 17(1), 32-45 (doi: 10.9767/bcrec.17.1.12366.32-45)

Permalink/DOI: <https://doi.org/10.9767/bcrec.17.1.12366.32-45>

1. Introduction

The oil and gas processing industry along with the petrochemical and chemical industries, is a labor-intensive production and it is accompanied by the formation of various wastes that have a negative impact on the environment. In order to involve alumina waste from polyeth-

ylene production for the industrial and economic circulation, the possibility of complex processing of this technogenic raw material into the followings is proved: 1) fresh adsorbent Uz-AD-1 for purifying hydrogen from chlorine-containing impurities at a naphtha reforming unit was proved [1]; 2) a component of carriers of catalysts for hydrotreating, prehydrotreating and demetallization of heavy oil feedstock [2]; 3) pseudoboehmite for the synthesis of an adsorbent of

* Corresponding Author.

Email: mi-shavkat@yandex.ru (S. Mamatkulov)

a protective layer for the process of oxidative conversion of hydrogen sulfide [3]. The adsorbent Uz-AD-1, which was developed by us, as well as its imported counterparts, is inevitably turned into a waste category after 1-2 years of operation. The solution to the problem of processing these wastes, containing a large amount of chemisorbed corrosive substances, is very important for enterprises where installations provide a halogenation procedure during the regeneration of reforming catalysts. Due to the huge demand for high-quality gasoline, we know about the hardware design [4,5] and the features of various naphtha reforming processes [6,7], the kinetics of reactions [8], causing an increase in the octane number of low-boiling hydrocarbons, the development and production of new catalysts [9–12] for implementation. The formation of acidic and metallic Pt centers, the mechanism of coke formation [13], the influence of a number of factors on the degree of deactivation of reforming catalysts [14], and optimization of the conditions for their regeneration [15] have been studied in detail. Information on the purposeful preparation of specific adsorbents for the auxiliary process of purification of hydrogen-containing gas from halogen-containing compounds is reflected mainly in patents [16–18], and insufficient attention has been paid to the disposal of spent adsorbents [19].

In this paper we present the results of thermochemical activation of the Axstrap-860 adsorbent, spent in the process of purifying a hydrogen-containing reforming gas of the fuel direction with an emphasis on recycling and waste-free technology of its regeneration. The role of hydrogen in oil refining, petrochemistry and organic chemistry can hardly be overestimated. Hydrogen at oil refineries (refineries) is obtained in the process of catalytic reforming, in which it is formed as a by-product and it is used as a reagent in the hydrodesulfurization of fuels and oils after purification. However, reforming hydrogen does not fully meet the needs of even hydrogenation processes, not to mention the large tonnage production of ammonia. As a result, in the mid-70s, in the midst of the first wave of the energy crisis, hydrogen energy was developed vigorously and it is produced purposefully [20]. Interest in hydrogen has not faded away to this day [21,22]. Technical hydrogen with a purity of 97-97 %vol, suitable for hydrotreating and hydrocracking, is produced by vapour conversion, either natural gas or straight-run gasolines [23]. Vapor conversion of methane is currently one of the basic processes in the chemical industry [24–26], so that inten-

sive research is being carried out to develop efficient and reliable fuel processors - generators of synthesis gas and hydrogen into fuel for power plants [27–29]. In order to implement the principle of "multi-fuel", *i.e.*, the conversion of various types of hydrocarbon raw materials into a mixture of H₂ and CO, Zyryanova *et al.* [29] selected NIAP-18, a catalyst for vapour and vapour-carbon dioxide conversion of natural gas. This is an industrial catalyst, tableted from a high-alumina carrier in the form of cylindrical rings, calcined at 1500 °C. The main active component of the catalyst is an inserted nickel oxide with 3.7 wt.% Ca and 0.5 wt.% Mg promoters. At the same time, the authors emphasize the need for further improvement of the catalyst in order to increase its coke resistance.

Previously, the coke deposits on K-38 (NiO/MgAl₂O₄) catalyst were absent, both in a laboratory unit and after 10 months of its operation as a frontal layer in the process of steam conversion of heavy refinery gases at the Gas Plant of PA Angarsknefteorgsintez. Therefore, the possibility of synthesizing magnesium-aluminum spinel [30] was simultaneously considered as a useful by-product in demand of various industries [31–35] during the production of a new adsorbent of chlorine-containing compounds based on the spent adsorbent Axstrap-860, unloaded from the adsorber of the naphtha reforming unit of the Bukhara Refinery.

2. Materials and Methods

For the complex processing of secondary aluminum-containing raw materials, the following reagents were used: the Axstrap-860 adsorbent spent in the process of cleaning off-gases from chlorine-containing compounds (Bukhara Refinery, Uzbekistan); NaOH, 25% NH₄OH and 65% HNO₃ (Navoiazot JSC, Uzbekistan); KOH (CHEMPACK, Russia), MgO (MAGNIKORM, Russia); Ni (NO₃)₂ 6H₂O (OJSC Ural Plant of Chemical Reagents, Russia).

The content of the main elements (aluminum, sodium, and chlorine) in solid waste adsorbents was determined using a scanning electron microscope EVOMA 10 (Zeiss). The porous characteristics and specific surface of the carriers and catalysts were determined using a Carlo Erba porosimeter by mercury penetration under pressure from 0 to 200 MPa. The concentration of aluminum in solutions was determined by complexometric titration, chloride ions on argentometric

titration, and sodium on flame photometry. The relative content of chlorinated oligomers in the sediments was estimated by the appearance of the 1270–1300 cm⁻¹ band when recording IR spectra in the incomplete internal reflection mode on a Nicolet S50 spectrometer. Diffraction patterns of the samples were obtained on a diffractometer (Empyrean Diffractometer), and thermograms on a HESON HS-TGA-103 derivatograph within the temperature range of 298–1273 K with a heating rate of 10 K/min. Electronic spectra of diffuse reflectance of indicators which were adsorbed to identify the main centers on the surface of the studied adsorbents, were recorded on a Hitachi-330 spectrometer [36,37].

The ability of the obtained adsorbents to form chlorinated oligomers was assessed by the appearance of chlorhexane (band 850-650 in the IR spectrum) in the composition of gaseous reaction products formed by passing a gas mixture - hydrogen or dried nitrogen containing 7-8 g/m³ HCl, 10 g/m³ hexane, and 2.5 g/m³ hexene-1, through 15 cm³ of the adsorbent at a rate of 20 L/h at 323–328 K for more than 200

hours in a circulation mode. In addition, the changes in the IR spectrum of the adsorbents were considered before and after the passage of the specified model mixture in a cyclic mode.

The obtaining a new Uz-AD-6 adsorbent was carried out in several stages, taking into account the uneven distribution and chemical properties of adsorbed substances in the spent Axstrap-860. Hydrogen and hydrocarbons in the composition of the gas being purified were weakly bound to the adsorbent material (mainly physical adsorption) and were easily displaced from its surface by polar HCl and H₂O molecules during the adsorption process. Chemisorption, *i.e.* adsorption with the formation of new chemical compounds proceeded while interacting with alkaline substances, and then with aluminum hydroxides in the composition of fresh Axstrap-860 (Figure 1, diffractogram 3) according to reactions 1-4:

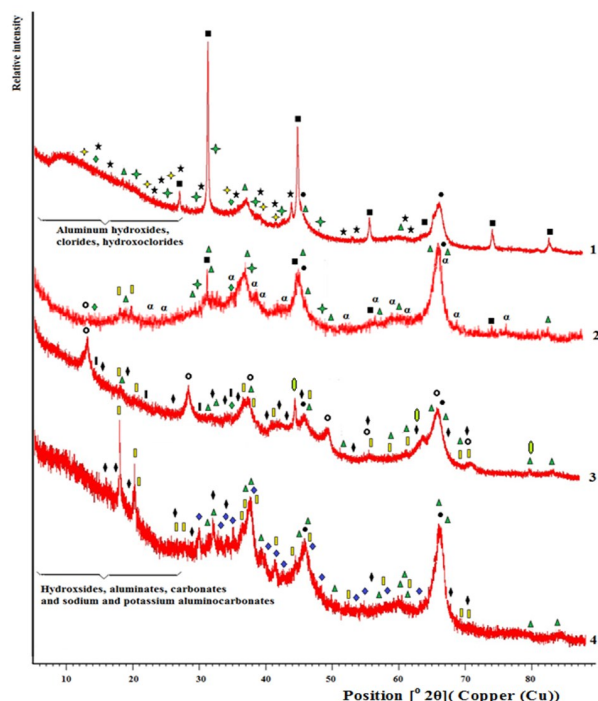
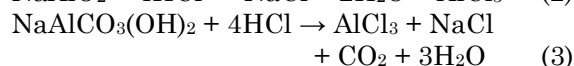
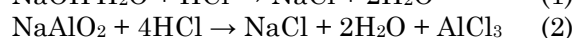


Figure 1. Diffraction patterns of samples at different stages of preparation of the modified adsorbent Uz-AD-6. (1)-spent Axstrap-860; (2)-washed and dried Axstrap-860; (3) - fresh Axstrap-860; (4)-Uz-AD-6. ● - γ -Al₂O₃, ▲ -Al_{10.66}O₁₆, ■ -NaCl, ▭ -Al(OH)₃, ○ -AlOOH, α -α-Al₂O₃, ◆ -Na₂CO₃, ♦ -NaAlCO₃(OH)₂, ▨ -NaOH·H₂O, ◊ -MgO, + -calcium chloride, * -magnesium chloride.

The maximum concentration of sodium and aluminum chlorides was observed in the frontal layer of an industrial adsorber and gradually decreased until there was no AlCl₃ at the outlet. Chlorides and hydroxochlorides of aluminum were formed during the interaction of boehmite in the composition of a fresh adsorbent with HCl, and NaCl with surface X-ray amorphous sodium aluminates (Figure 1). The contact of the spent Axstrap-860 with water was accompanied by partial (15–20 %mass) destruction of granules up to a powdery state due to their hygroscopicity. Therefore, the spent adsorbent was first washed with water, the whole granules were separated on a sieve, they were dried and calcined at 700–710 K to remove AlCl₃ residues and coke-like deposits [1] (Table 1). Then the calcined granules were impregnated with an alkaline solution containing 195 g/L NaOH and 45 g/L KOH, taking into account the moisture absorption of 47-55 %mass, they were dried in air and put in a muffle furnace at a temperature not higher than 570 K. After settling the wash water suspension, a clear solution containing NaCl, chlorides and aluminum hydroxochlorides was separated by decantation. Then this solution was sent to separate the corresponding salts as useful by-products - sodium and aluminum chlorides. Meanwhile, the sediment consisting of fine

Table 1. Elements detected during scanning of various areas of the spent adsorbent granules - Axstrap-860 on EVOMA electron microscope.

No	Calculated chemical composition (% wt.) based on the results of elemental analysis	Content, % wt						
		C	O	Na	Al	Cl	Mg	Ca
Volume of granules								
144	59- AlOOH, 18.3- NaCl, 15.8-Al ₂ O ₃ , 6.6-AlCl ₃ ·6H ₂ O	-	42.48	7.19	36.17	14.16	-	-
145	49.7Al ₂ O ₃ , 19.7 AlOOH, 18.1 NaCl, 9 AlCl ₃ ·6H ₂ O	-	41.32	7.13	36.37	15.19	-	-
146	37.8 Al ₂ O ₃ , 32.6 Al(OH) ₃ , 18.3 NaCl, 7.3 AlCl ₃ ·6H ₂ O, 1.3 MgCl ₂	-	41.80	7.23	35.14	15.48	0.34	-
147	47.6 Al ₂ O ₃ , 25 Al(OH) ₃ , 19.2 NaCl, 5.6 AlCl ₃ ·6H ₂ O, 0.13CaCl ₂	-	42.08	7.55	34.88	15.04	-	0.45
148	38 Al ₂ O ₃ , 32.8 AlOOH, 19 NaCl, 7.7 AlCl ₃ ·6H ₂ O, 1.3% MgCl ₂	-	41.08	7.55	36.10	15.28	-	-
On the surface of the granules								
149	53.6 Al ₂ O ₃ , 22.2 NaCl, 11.6 CaCl ₂ ·2H ₂ O, 10.7Mg ₂ (OH) ₃ Cl·4H ₂ O	-	35.73	8.78	28.42	21.18	2.64	3.24
150	67.3 Al ₂ O ₃ , 16.7 NaCl, 5 Mg ₂ (OH) ₃ Cl·4H ₂ O, 4.7CaCl ₂ ·2H ₂ O, 4.7 AlCl ₃ ·6H ₂ O	-	39.05	6.59	36.21	15.59	1.24	1.32
151	44.6 Al ₂ O ₃ , 20.8 NaCl, 15.3 AlOOH, 8.34 AlCl ₃ ·6H ₂ O, carbon	5.3	38.38	8.20	31.59	16.53	-	-
152	46.3 Al ₂ O ₃ , 19.6 AlOOH, 19.1 NaCl, 13.2 AlCl ₃ ·6H ₂ O	-	39.67	7.50	35.16	17.68	-	-
153	67.6 Al ₂ O ₃ , 17.3 NaCl, 11.4 AlCl ₃ ·6H ₂ O, carbon	1.83	38.43	6.80	37.15	15.80	-	-
On the surface of washed granules								
196	95.2 AlOOH, 0.67 NaAlO ₂ , 0.58 NaCl	-	55.43	0.42	43.80	0.35	-	-
197	87.56 AlOOH, 9.44 Al ₂ O ₃ , 0.86 NaCl, 0.71 NaAlO ₂	-	53.64	0.54	45.3	0.52	-	-

The numbers of the electronic images in the figure

particles of $\gamma\text{-Al}_2\text{O}_3$ and $\text{Al}(\text{OH})_3$ in a mixture with crumbs of destroyed granules, and containing no more than 3% Cl^- mass, served as a raw material for obtaining pseudoboehmite. For this purpose, the sediment was dissolved in nitric acid with a density of 1.26–1.27 g/mL at a temperature of 360–365 K. Then the aluminum nitrate solution was decanted into a vessel equipped with a stirrer after cooling.

The deposition of aluminum monohydroxide was carried out with a 25 %mass. NH_4OH solution maintaining pH of 7–7.5. The maturation of sediments, subsequent filtration and washing on a nutsch filter was carried out at a temperature of 290–295 K, and drying to a powdery state at 360 K. The $\gamma\text{-Al}_2\text{O}_3$ adsorbent was obtained by molding dried pseudoboehmite followed by calcining at 825 K and this adsorbent was intended for removing droplet moisture from wet process gases. Aluminum monohydroxide powder in the form of a gel-like pseudoboehmite with a crystal size of 20–30 Å, was thoroughly mixed with magnesium oxide and water in an atomic ratio of $\text{Mg}:\text{Al} = 1:2$ for 4–5 hours for destructive-epitaxial interaction in order to obtain a bidispersed magnesium-aluminum spinel. As a result of the partial dissolution of poorly soluble reagents in water, there was a gradual formation of magnesium hydroxoaluminates with a pseudoboehmite morphology [38]. Then the mass was mixed again, evaporated to a consistency suitable for molding by extrusion into Raschig rings with a diameter of 15×2 mm. Having dried in air, the pellets were heated by raising the temperature in a muffle furnace at a rate of 20–30 K/h up to

1440–1450 K with holding at this temperature for 5 hours.

The $\text{NiO}/\text{MgAl}_2\text{O}_4$ catalyst was prepared by moisture absorption impregnation of magnesium-aluminum spinel granules with a 58% aqueous solution of $\text{Ni}(\text{NO}_3)_2 \cdot 6\text{H}_2\text{O}$, the catalyst after calcination at 873K contained 12 %mass. NiO (0.26 M NiO / 1 M MgAl_2O_4). The acid reference catalyst obtained similarly by impregnation of $\gamma\text{-Al}_2\text{O}_3$ from fresh pseudoboehmite contained 0.19 M NiO/1 M $\gamma\text{-Al}_2\text{O}_3$. The activity of the catalysts was evaluated in a laboratory setup by the degree of hexane conversion in a model mixture of hexane and water vapors ($\text{H}_2\text{O}:\text{C} = 3:1$ mol/g-atom) in a helium flow, and the selectivity by the amount of coke deposits. The process was carried out at a temperature of 773 K, at a pressure of 0.1 MPa, a space velocity of 4 h⁻¹ for liquid hydrocarbon, and a hexane:helium ratio of 1:40. The composition of the model mixture and gaseous reaction products, as well as the chemisorption of hydrogen during the temperature-programmed reduction of the samples, was determined on a Chrom 5 chromatograph.

3. Results and discussion

In the process of optimizing the preparation conditions for Uz-AD-6 from the spent adsorbent Axstrap-860 (specific surface area - 70–177 m²/g), the necessary and sufficient degree of removal of chlorine ions was revealed: from 5–20 %mass, Cl up to 1–2 %mass, and residual chlorine after completion of the water treatment and calcination procedure. More than half of the chemisorbed substances remain in the test sample with a

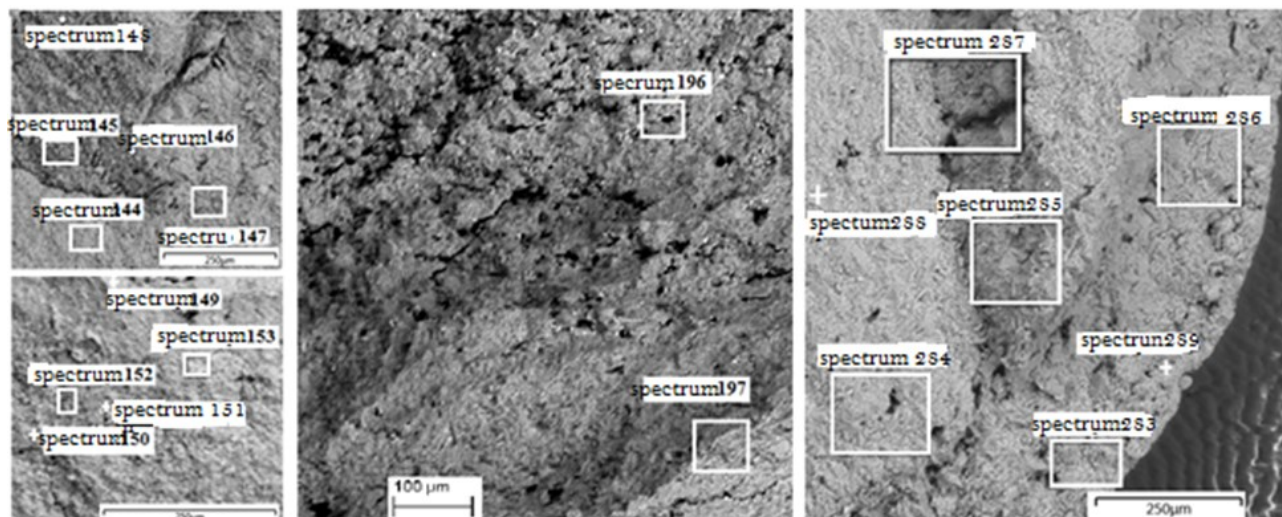


Figure 2. Photo of a cut of the spent adsorbent granules: on the left (top - the middle of the granule, below - the surface layer), the granule after washing with water and calcining in the center, and on the right - finished Uz-Ad-6.

washing time of less than 10 hours. However, treatment with water for more than 24 hours is accompanied by the formation of an excessive amount of a low-concentrated suspension that is not suitable for further processing. The concentration of residual chlorine identified after calcining the washed granules in the temperature range of 670–570 K was below 0.5 %mass, and the specific surface area reached 280-300 m²/g due to the sublimation of aluminum chloride and burnout of carbon deposits [1] (Table 1). A feature of the morphology of the studied samples is the formation of a relatively loose layer with a thickness of about 250 μm and a denser middle part (Figure 2, photo on the right).

This phenomenon is explained by the expansion of pores and microcracks due to the extraction of the products of the interaction of chlorine-containing compounds from them with X-ray amorphous sodium aluminates and boehmite in the composition of the adsorbent. A powerful halo in the range of small angles $2\theta = 7.6^\circ\text{--}7.82^\circ$ ($d = 11.6\text{--}11.3 \text{ \AA}$) witnesses the presence of surface sodium aluminates in fresh Axstrap-860. There are lines of 100% intensity of the phases NaAl₁₁O₁₇, NaAl₇O₁₁, NaAl₅O₈ and NaAl₃O₆ (Figure 1, diffractogram 3). Weaker halos in the range of $2\theta = 15.5^\circ\text{--}16.6^\circ$, $19.6^\circ\text{--}26.8^\circ$, $31.0^\circ\text{--}35.8^\circ$, $40.5^\circ\text{--}45.9^\circ$, $57.9^\circ\text{--}63.0^\circ$ and $66.0^\circ\text{--}68.8^\circ$ ($d = 5.69\text{--}5.30$, $4.5\text{--}3.3$, $2.88\text{--}2.5$, $1.588\text{--}1.47$ and $1.41\text{--}1.36 \text{ \AA}$) located between the intense lines of boehmite and they can be attributed to the manifestation of not only sodium polyaluminates, but also NaAlO₂ and 2NaAlO₂·3H₂O.

The solid crust covering the pore walls of the spent Axstrap-860 (Figure 2, bottom left photo; Table 1) consists of coarse crystalline NaCl ($d = 3.32$, 2.88 , 2.033 , 1.66 , 1.44 , 1.284 and 1.17 \AA) and sometimes anhydrous AlCl₃, weakly crystallized AlCl₃·6H₂O (broad lines with $d = 6.0$, 5.2 , 3.89 , 3.69 , 3.29 , 2.57 , 2.3 , and 2.05 \AA). An intense halo in the range of $2\theta = 7.7\text{--}28^\circ$ (Figure 1, diffractogram 1) indicates the presence of a mixture of several hydrolyzed forms of polynuclear hydroxo complexes of variable composition, which are expressed by the general formula [Al(OH)_{3-x}Cl_y]_n, where x varies within 0–3 [1].

In the diffraction patterns of the heavily hardened Axstrap-860 (frontal layer), the AlCl₃·6H₂O and AlCl₃ lines appear very well, as well as in the one stripped off and dried aqueous extract both before and after separation of NaCl crystals. When heated to a temperature of 455 K, the spent Axstrap-860, especially the dried aqueous extract, AlCl₃ sublimates. According to

the results of elemental analysis, the composition of the dry extract on average corresponds to the formula Al₂(OH)_{5.2-5.0}Cl_{1.0-0.8}, *i.e.* it is close to the composition to aluminum pentahydroxochloride - a coagulant with the maximum coagulating ability among other aluminum hydroxochlorides.

We can assume the presence of magnesium and calcium chlorides based on the results of computer processing of diffraction pattern 1 in Figure 1: CaCl₂– $d = 4.49$, 3.46 , 3.05 , 2.85 , 2.33 , 2.24 , 2.09 , 1.9 , 1.79 , 1.68 \AA , CaCl₂·6H₂O– $d = 6.9$, 12.8 , 3.93 , 3.41 , 2.78 , 2.58 , 2.27 , 2.16 \AA , MgCl₂– $d = 5.9$, 2.94 , 2.55 , 1.80 \AA , MgCl₂·6H₂O– $d = 5.8$, 4.10 \AA . Indications of the presence of magnesium and calcium compounds are also found in the diffractograms of fresh Axstrap-860 (Figure 1, diffractogram 3).

Complexometric titration with a solution of the sodium salt of ethylenediaminetetraacetic acid, first at pH 12-13 in the presence of murexide as an indicator, confirmed the presence of Ca²⁺ cations, and then at pH = 10 Mg²⁺ in the composition of fresh and used Axstrap-860. The presence of inclusions of calcium and magnesium compounds in some samples was also recorded on a scanning electron microscope (Figure 2, Table 1). In the Axstrap-860 used, the content of Na and Cl in the surface layer of the granules was in the range of 4.3–5.4 and 8.5–9.3% of the mass, respectively, and in the middle of the granules is slightly less: 2.9–3.3 and 1.2–1.5% of the mass.

In the process of alkaline modification, due to the presence of transport channels with a width of about 12 μm, which are clearly visible on the cut of the granule (Figure 2, photo in the center), the joint solution of sodium and potassium hydroxides freely penetrated deep into the granules, purified from the bulk of substances (NaCl, AlCl₃·xH₂O and [Al(OH)_{3-x}Cl_y]_n), which blocked the pores of the spent adsorbent. The specificity of the obtained adsorbent is the almost complete absence of the phase of aluminum monohydroxide, which is replaced by aluminum trihydroxide - gibbsite. When statistically processing the results of elemental analysis of a series of Uz-AD-6 samples, the concentration in the outer layer of granules was within 6.5-9.2 Na% and 1-5 K%, and in the inner volume, respectively, 2.5-3.5 Na% and 0.5-0.7 - 1.5 K% (Table 2). Based on the molar ratio of carbonate carbon and alkali metals in the composition of representative samples (10 g each), it was concluded that the amorphous phase of sodium aluminate Na₇Al₃O₈ prevails over sodium and potassium monoaluminates. The finished Uz-AD-6 contains water-soluble sodium

Table 2. Elements detected during scanning of various areas of granules of the obtained adsorbent - Uz-AD-6 on EVOMA electron microscope.

No	Calculated chemical composition (%wt) based on the results of elemental analysis	Content; %wt								
		C	O	Na	Al	Cl	Mg	Ca	K	Fe
283	41.7 Al(OH) ₃ , 37.2 Al ₂ O ₃ , 13.6 NaOH, 2.38 K ₂ CO ₃ , 2.36 NaAlCO ₃ (OH) ₂ , 0.88 Na ₂ CO ₃ , 0.24 NaCl	0.5	51.48	8.89	35.17	0.15	-	-	1.35	-
284	72 Al ₂ O ₃ , 13.9 Al(OH) ₃ , 7.1 NaOH, 3.5Na ₂ CO ₃ , 2.4 K ₂ CO ₃ , 0.19 Fe ₂ O ₃ , 0.15 KOH	0.6	48.94	5.74	43.13	-	-	-	1.46	0.13
285	64.7 Al ₂ O ₃ , 13.9 Al(OH) ₃ , 7.07 Na ₂ CO ₃ , 5.44 NaOH, 0.44NaCl	0.8	53.19	6.45	39.29	0.27	-	-	-	-
286	66.1 Al ₂ O ₃ , %, 16.7Al(OH) ₃ , 9.4 NaOH, 2.12 Na ₂ CO ₃ , 1.82 K ₂ CO ₃ , 0.24 NaCl	0.4	50.86	6.56	41.0	0.15	-	-	1.03	-
287	63.3 Al ₂ O ₃ , 20.8 Al(OH) ₃ , 9.54 Na ₇ Al ₃ O ₈ , 4.42 Na ₂ CO ₃ , 0.19 Fe ₂ O ₃ , 0.16 NaCl	0.5	49.98	6.13	43.10	0.1	-	-	-	0.19
Volume of granules										
The images are not given										
	51.3 Al ₂ O ₃ , %, 32.7 Al(OH) ₃ , 3.98 Na ₂ CO ₃ , 2.66 MgCO ₃ , 1.4 Na ₇ Al ₃ O ₈ , 0.69 NaCl, 0.58 CaCO ₃	0.9	55.28	2.62	39.27	0.42	0.76	0.23	0.52	-
	58.12 Al ₂ O ₃ , 33.3 Al(OH) ₃ , 4.37 Na ₇ Al ₃ O ₈ , 1.35 KAlO ₂ , 0.85 NaCl, 0.17 Fe ₂ O ₃	-	53.82	2.54	42.77	0.21	-	-	0.54	0.12
	56.67 Al ₂ O ₃ , 29.7 Al(OH) ₃ , 3.19 Na ₇ Al ₃ O ₈ , 2.36 NaOH, 0.86 NaCl,	-	51.20	3.12	44.4	0.52	-	-	0.76	-

and/or potassium carbonates, in contrast to $\text{NaAlCO}_3(\text{OH})_2$ identified in fresh Axstrap-860. The presence of insoluble sodium carboaluminate $\text{NaAlCO}_3(\text{OH})_2$ was confirmed by the reaction of CO_2 release upon addition of hydrochloric acid solution to the adsorbent sample after preliminary removal of soluble sodium carbonates by aqueous extraction. Carbonate carbon in the composition of sodium, calcium and magnesium carbonates and/or carboaluminates was estimated by the amount of CO_2 released during the interaction of a sample of the adsorbent composition with hydrochloric acid.

In addition to 0-0.3% mass. residual chlorine, when viewed through an electron microscope, point inclusions of corrosive iron are observed, which cannot be removed by water and heat treatment. Calcium and magnesium recorded in some areas indicate incomplete removal of chlorides at the washing stage and / or the introduction of hardness salts with tap water.

In general, during the complex processing of 50 kg of spent Axstrap-860, 34.2 kg of a new Uz-AD-6 adsorbent were obtained, 2.4 kg of crystalline NaCl and 13.5 kg of dried aluminum

hydrochloride were isolated from the wash water, and 6.8 kg of aluminum hydroxide of pseudoboehmite modification was obtained from the insoluble residue of the suspension by reprecipitation. Our attempt to use aluminum hydroxide obtained as a by-product in the production of the Uz-AD-6 adsorbent for the synthesis of magnesium-aluminum spinel showed that freshly precipitated pseudoboehmite AlOOH stabilized by residual NH_4^+ , NO_3^- ions and nitrohydroxocomplexes readily undergoes destructive epitaxial transformations $\text{AlOOH-MgO-H}_2\text{O}$.

In the IR spectra of the dried mass intended for the formation of Raschig rings, an intense band at 1390 cm^{-1} , corresponding to nitrate ions, remains, along with the appearance of a series of bands indicating the formation of magnesium hydroxoaluminates: a narrow band at 420 cm^{-1} and a wide band with maxima at 480 and 580 cm^{-1} . That is, partial dissolution of MgO with the formation of Mg^{2+} and OH^- ions, their subsequent adsorption on the surface of loose particles of less soluble AlOOH with a gradual rearrangement of its crystal lattice up to complete transformation into magnesium hydroxoaluminate. This follows from the disappearance in the diffractogram of the resulting paste (Figure 3, diffractogram 1) of broad lines characteristic of weakly crystallized pseudoboehmite ($d = 6.10, 3.16, 2.34, 1.86, 1.85, 1.66\text{ \AA}$) and narrower lines from the initial magnesium oxide ($d = 2.43, 2.09, \text{ and } 1.35$), instead of which a set of lines with ($d = 8.03, 7.61, 4.05, 4.01, 3.82, 2.614, 1.97, 1.515, \text{ and } 1.493\text{ \AA}$) belonging to magnesium hydroxoaluminates is observed. Due to the epitaxial growth of new formations, the crystals of the newly formed phase have dimensions of the same order of magnitude as the AlOOH crystals. Upon completion of the reactions in the $\text{AlOOH-MgO-H}_2\text{O}$ system, a paste is formed from partially intergrown crystals of magnesium hydroxaluminates. After calcination, due to the removal of gaseous products, the size of the MgAl_2O_4 crystals becomes smaller, but their configuration is retained during dehydration. The morphological feature of the obtained spinel is the formation of grape-like particles with $1\mu\text{m}$ sizes, which determine its biporous structure and maintain high mechanical strength upon repeated heating to 1000 K and rapid cooling. A thermographic study revealed a complete disappearance of the exothermic effect at 543 K observed on the DTA curve of the synthesized pseudobemite due to the thermal decomposition of the incompletely washed ammonium nitrate. In addition, a shift of the

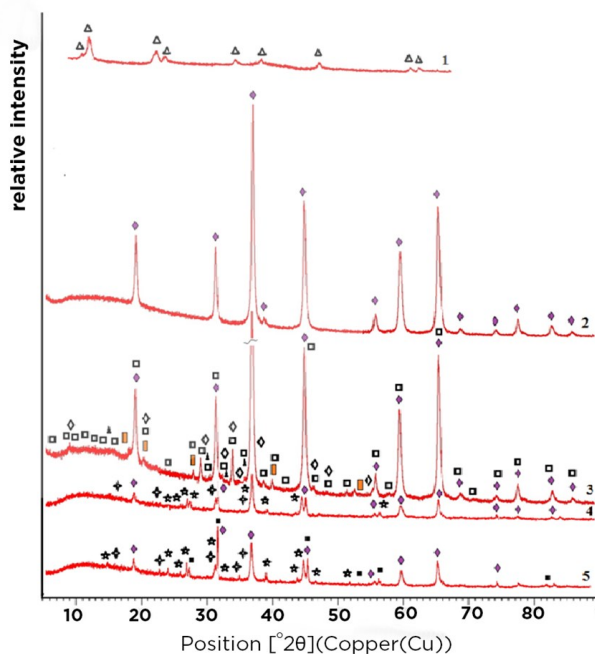


Figure 3. Diffraction patterns of (1) magnesium hydroxoaluminate, (2) MgAl_2O_4 , (3) $\text{MgAl}_2\text{O}_4\cdot\text{NaOH}$; after exposure to saturated vapors of a mixture of hydrochloric acid, tetrachlorethylene and hexene-1 of the samples: (4) MgAl_2O_4 , (5) $\text{MgAl}_2\text{O}_4\text{-NaOH}$. \blacklozenge - MgAl_2O_4 , \blacktriangle -magnesium hydroxoaluminates, \blacksquare -magnesium carbonates, \blacklozenge -sodium carbonates, \blacksquare -bayerite, \blackplus -magnesium chlorides, \blackstar -chlorides aluminum, \blacksquare -sodium chloride, \blacktriangle -sodium hydroxide.

stretched endothermic effect around 665 K was observed, characteristic of AlOOH dehydration with transition into γ -Al₂O₃ to the low-temperature region, as well as the endothermic effect from the transformation of Mg(OH)₂ into MgO at 855 K. Instead the following are observed: a deep endo-effect at 400-408 K, and less intense endothermic effects at 620 and 795 K accompanied by mass loss of 37, 20, and 4%, respectively. According to the TH curve, the dehydration processes of magnesium hydroxoaluminates end around 870 K with the formation of X-ray amorphous products. At the further rise in temperature up to 1440-1450 K the degree of crystallinity increases and sintering of MgAl₂O₄ crystals begins. But as in the case of industrial pseudobemite [30], spinel particles obtained through destructive-epitaxial transformations present open-worked formations, resulting in high strength - 380-390 kg/cm², biporous structure and specific surface area of 28-32 m²/g. After calcination at 1450 K, the volume of micropores measuring 30-100 Å was 0.16 cm³/g, and the volume of macropores measuring 1000-30000 Å was 0.26 cm³/g.

In the diffractogram of the calcined sample, in contrast to the magnesium-aluminum spinel prepared by the same technology, but from industrial aluminum hydroxides with crystal sizes 50-75 Å [30], only magnesium aluminate was identified. The crystal phase MgAl₂O₄ corresponded to lines with $d = 4.657, 2.858, 2.453, 2.31, 2.008, 1.637, 1.55, 1.424, 1.3606, 1.27, 1.225, 1.162$ and 1.1271 Å. The most intensive lines with $d = 3.48, 2.55, 2.08, 1.74$ and 1.61 Å, typical for α -Al₂O₃ and with $d = 2.10, 1.485$ and 1.266 Å, corresponding to MgO, were absent (Figure 3, diffractogram 2). Acidic centers with

pKa $\leq +3.8$ provoking coking were not identified on the spinel surface, the main centers with pKa about 9.3 prevailed, and also stronger main centers with pKa $> +10.3$ were found.

The NiO/MgAl₂O₄ catalyst, similarly to the K-38 catalyst, contained nickel mainly in the form of a nonstoichiometric oxide - NiO_{1+x}, which is capable of chemisorbing hydrogen at a temperature of 710-860 K with the formation of Ni²⁺ centers, which largely determine the selectivity of the steam conversion of hydrocarbons. MgAl₂O₄ and all adsorbents studied in the article did not chemisorb the hydrogen under conditions of temperature-programmed reduction within the temperature range of 295-970 K, only physical adsorption was observed.

According to the results of testing the synthesized NiO/MgAl₂O₄ catalyst under severe conditions similar to the testing of K-38 catalyst, which allow predicting catalytic properties, it was shown that the degree of hexane conversion % with the formation of gaseous products (H₂, CO, CO₂, CH₄) was at least 90% mass. in the model process of steam conversion of liquid hydrocarbons. Analysis of carbonaceous deposits revealed that the coke did not exceed 0.05 % mass, while the amount of coke reached 0.35 % mass on the NiO/ γ -Al₂O₃ catalyst of "acidic" nature.

Besides, in order to reveal possibility of application of magnesium-aluminum spinel as a protective (distributive) layer in adsorbents for gas purification from halide compounds in the presence of a lot of water vapor its modification by moisture absorption by 24 % sodium hydroxide solution was carried out. From some displacement of MgAl₂O₄ lines in the diffractogram in Figure 3 we made an assumption

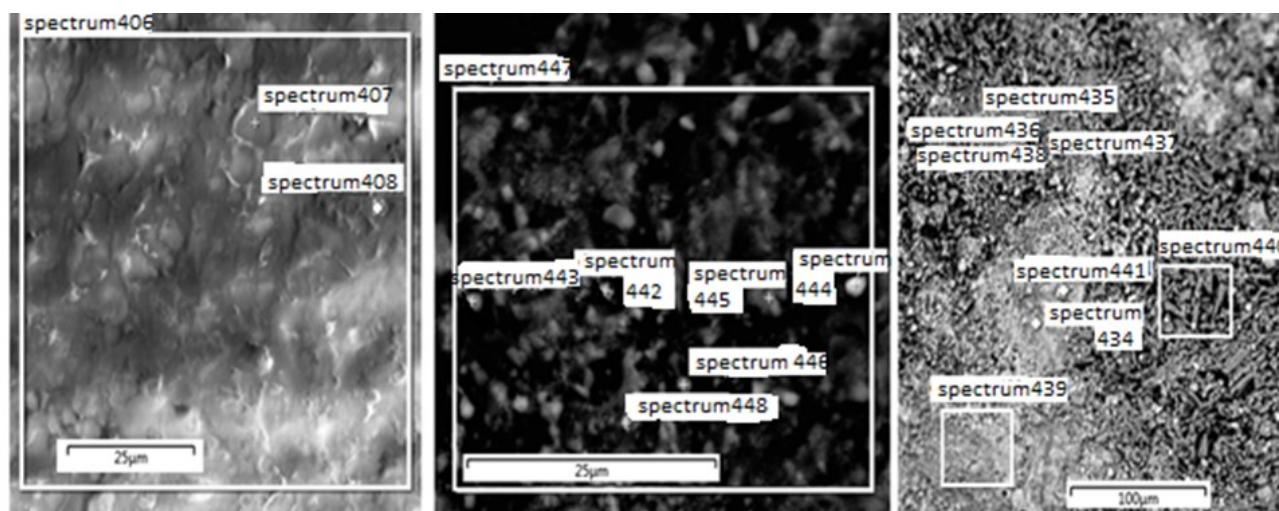


Figure 4. Photo of the surface of the original MgAl₂O₄ pellet (left); modified with sodium hydroxide (center and right side).

Table 3. Elements detected during scanning of various areas of granules based on magnesium-aluminum spinel on EVOMA electron microscope.

No	The most probable chemical compounds on the surface of the granules (wt%, calculated from the results of elemental analysis)	Content; %wt					
		C	O	Na	Al	Mg	Ca
On the surface of granules- MgAl ₂ O ₄							
406	91.6 MgAl ₂ O ₄ , Al ₂ O _{3-x}	-	41.96	-	42.55	15.9	-
407	86.8 MgAl ₂ O ₄ , Al ₂ O _{3-x}	-	45.22	-	40.10	14.7	-
408	78.6 MgAl ₂ O ₄ , Al ₂ O ₃	-	47.81	-	38.91	13.8	-
On the surface of granules - MgAl ₂ O ₄ -Na							
434	67MgAl ₂ O ₄ , 21.4 Na ₇ Al ₃ O ₈ , 5.39NaOH	-	45.99	12.50	30.18	11.3	-
435	36.68 Na ₇ Al ₃ O ₈ , 35.5 MgAl ₂ O ₄ , 5.1NaOH, 3.83Mg(OH) ₂ , xH ₂ O	-	51.85	18.97	21.53	7.64	-
436	46.63 Na ₇ Al ₃ O ₈ , 14.79 MgAl ₂ O ₄ , 13.33 Al(OH) ₃ , 11.99 Mg(OH) ₂ , xH ₂ O	-	51.38	20.29	20.63	7.70	-
437	45.73 MgAl ₂ O ₄ , 22.3 NaOH, 14.8 Na ₇ Al ₃ O ₈ , xH ₂ O	-	51.91	19.56	20.80	7.73	-
438	42.47 NaAlO ₂ , 16.98 MgAl ₂ O ₄ , 13.04 NaOH, 12.02 Mg(OH) ₂ , xH ₂ O	-	51.75	19.69	20.54	8.02	-
439	27.52 MgAl ₂ O ₄ , 23.21 Na ₇ Al ₃ O ₈ , 17.1NaOH, 14.1 Al(OH) ₃ , 6.84 Mg(OH) ₂ , xH ₂ O	-	51.59	20.20	20.63	7.58	-
440	44.2 MgAl ₂ O ₄ , 24.04NaOH, 14.8 Na ₇ Al ₃ O ₈ , xH ₂ O	-	51.85	20.62	20.05	7.47	-
441	46,76 MgAl ₂ O ₄ , 25.35 NaOH, 11.56 Na ₇ Al ₃ O ₈ , xH ₂ O	-	51.79	19.98	20.33	7.90	-
442	33.45 NaAl ₁₁ O ₁₇ , 31.48 MgAl ₂ O ₄ , 2.5 NaOH, 1.47 Mg(OH) ₂ , xH ₂ O	-	62.52	2.78	28.75	5.95	-
443	68.04 MgAl ₂ O ₄ , 12.4NaAlO ₂ , 7.07 Na ₂ CO ₃ , 3.75 Al(OH) ₃ , 3.08 MgCO ₃ , xH ₂ O	1.24	48.53	6.55	31.30	12.8	-
444	35.97 NaHCO ₃ , 24.87 NaAl ₅ O ₈ , 14.02 MgAl ₂ O ₄ , 8.2 Al(OH) ₃ , 8 Al ₂ O ₃ , MgCO ₃ ,	6.2	53.21	11.97	24.25	4.37	-
445	31.2 Al ₂ O ₃ , 29.87 MgCO ₃ , 19.85 NaHCO ₃ , 16.22 Na ₇ Al ₃ O ₈	7.07	51.92	12.60	20.04	8.37	-
446	48.88 MgAl ₂ O ₄ , 22.38 Na ₇ Al ₃ O ₈ , 10.15 Na ₂ CO ₃ , 7.28 Al(OH) ₃ , xH ₂ O	1.15	50.34	14.14	26.12	8.26	-
447	55.91MgAl ₂ O ₄ , 24.03 Na ₇ Al ₃ O ₈ , 6.29 NaOH, xH ₂ O	-	49.95	14.08	26.52	9.45	-
448	25.86 Al ₂ O ₃ , 23 NaHCO ₃ , 18.7 MgCO ₃ , 12.3 CaCO ₃ , 3.26 elemental carbon, xH ₂ O	12.3	52.03	6.37	13.69	5.33	10.2

about the introduction of Na⁺ ions into the crystal lattice of the magnesium-aluminum spinel. Appearance of separate distinct lines with $d = 3.18, 3.053, 2.75, 2.64, 2.31, 2.2475, 1.954, 1.861, 1.766, 1.7288, 1.632, 1.586 \text{ \AA}$ from crystalline phases that can be assigned to carbonates: Na₂CO₃, Na₂CO₃·7H₂O, MgCO₃·2H₂O, Mg₂(OH)₂CO₃·3H₂O, and Mg₅(CO₃)₄(OH)₂·5H₂O and halo in the low angle region with 2θ from 5.8 to 18°, corresponding to the most intense lines of magnesium carbonates, also indicates the migration of Mg²⁺ ions into the liquid phase during modification with subsequent interaction with atmospheric CO₂. The above was confirmed by elemental analysis (Figure 4, Table 3) by the appearance of carbon in the composition of some sections of MgAl₂O₄ modified with sodium hydroxide. Fluctuations in the amount of carbon in the composition of the studied samples, not correlated with the content of alkali and alkaline earth metals, can be explained by the variation in the amount of compounds formed and their uneven macro-distribution.

Testing the type of surface centers revealed that 48% of pellets taken at random during adsorption from benzene solution ionized phenolphthalein molecule and acquired bright crimson color, 37% were colored in a slightly pink color ($pK_a > +9.3$), and the rest remained white. In accordance with the study [36] about half of the alkali metal hydroxides in the process of modification turned into a highly basic aluminate - Na₇Al₃O₈ ($pK_a > +9.3$). From them one third of granules, as well as their separate sites (Figure 4, spectra No 435-441), containing an admixture of unreacted NaOH were capable to ionize thymolphthalein molecule, getting blue color characteristic for the main form of this indicator ($pK_a > +10.3$). Appearance of

slightly pink coloring of the main form of adsorbed phenolphthalein indicated formation of crystalline Na₂CO₃·2.5H₂O (Figure 3, diffractogram 3, Figure 4 spectra No 443-446, 448.) in addition to other sodium and potassium carbonates and monoaluminates with main centers of moderate strength ($pK_a \approx 8.3-9.3$). White coloration of granules after adsorption of phenolphthalein ($pK_a \geq +8.3$), indicated the formation of sodium polyaluminates with low mass ratio Na:Al, namely NaAl₁₁O₁₇, NaAl₇O₁₁ and NaAl₅O₈ (Figure 4 spectra No 434, 442, 447). The results of studies of adsorption properties of samples based on the used adsorbent Axstrap-860 and a by-product of its processing are shown in Table 4, which shows that the new adsorbent obtained by processing the used adsorbent in its adsorption characteristics is close to the fresh Axstrap-860, designed for gas purification from halide compounds.

Under identical experimental conditions, adsorbents modified with alkali metal hydroxides did not catalyze the formation of chlorinated hydrocarbons. In the IR spectrum of these samples, after the completion of the experiment, an increase in the intensity of broad bands in the range of 3325–3000, 1643–1585, and 527–493 cm⁻¹, characteristic for the initial adsorbents, was observed, and it is indicated the presence of adsorbed hydrocarbons, including hexene along with the appearance of a series of new inflection points at 1175–1205, 1055–1060, 980–960, 910–915, and 660–72 cm⁻¹.

In contrast to them, already at the initial stage, on the γ -Al₂O₃ and MgAl₂O₄ adsorbents, the chemisorption of HCl was accompanied by a chemical reaction with aluminum oxide and by the formation of a strong Lewis acid - AlCl₃.

Table 4. Dynamic adsorption capacity (g of adsorbate /100 g adsorbent) recorded after flowing through 10 cm³ of adsorbent a mixture of nitrogen and model substances at a rate of 20 L/h at 300 K.

Sample	Capacity of chloride*	Absorbate capacity before a "breakthrough"; g/100 g		
	8 g/m ³ – HCl, 2 g/m ³ – C ₆ H ₁₂ (Chloride-hexane)	7 g/m ³ dry HCl	7 g/m ³ 28 % hydrochloric acid	7 g/m ³ H ₂ O
Uz-AD-6	15.4 (no)	11.6	24.8	9.8
Axstrap-860	16.3 (none)	11.9	22.9	9.5
MgAl ₂ O ₄	9.2 (traces)	3.6	7.7	2.8
MgAl ₂ O ₄ -NaOH	14.4 (none)	13.3	14.8	4.4
γ -Al ₂ O ₃ from pseudoboehmite transformation	11.5 (yes)	9.3	17.4	5.6

*g Cl /100 g in circulation mode at 335 K.

As a consequence, in the IR spectrum of the gaseous reaction products, in addition to the bands of the model mixture, weak bands appeared within 850–550 cm⁻¹, attributed to the formation of chlorhexane. Chlorinated oligomers appeared only in the adsorbed state on the γ -Al₂O₃ surface in the form of a clear band at 1270–1300 cm⁻¹.

4. Conclusions

The studies of the features of the change in the chemical and phase composition of the alumina adsorbent, after the completion of the cycle of its operation in the process of removing chlorine-containing impurities from technological hydrogen, proved the expediency of its thermochemical modification with alkali metal hydroxides. The formation of highly basic aluminates of alkali metals and a satisfactory HCl adsorption capacity of the Uz-AD-6 adsorbent obtained by the complex processing of the used Axstrap-860 allow us to recommend it for reuse in the purification of hydrogen-containing gas at a naphtha reforming unit. Useful salts, including a coagulant for the purification of turbid water, were isolated from the liquid waste generated at the stage of removing chlorine-containing compounds. Pseudoboehmite and an alumina adsorbent were obtained as a by-product and this adsorbent is intended to remove droplet moisture from wet gases. The possibility of synthesis of magnesium-aluminum spinel resistant to thermal shock was found out, and it is suitable as a carrier for catalysts for steam conversion of hydrocarbons in accordance with its other characteristics.

Acknowledgements

This research was funded by Ministry of innovative development of the Republic of Uzbekistan, grant number FZ-2019-06066 and MUK-2021-45.

References

- [1] Yunusov, M.P., Nasullaev Kh.A., Gulomov Sh.T., Isaeva N.F., Mustafaev B.D., Rakhimjanov B.B., Khodjiev R.G. (2020). Analysis of the results of experimental sorbent for chloride compounds removal. *Chemical Problems*, 3(18), 366–375. DOI: 10.32737/2221-8688-2020-3-366-375
- [2] Yunusov, M.P., Djalalova, Sh.B., Nasullaev, Kh.A., Isaeva, Sh., Mirzaeva, E.I. (2016). New catalytic systems for hydrofining and dearomatization processes of oil fractions. *Catalysis for Sustainable Energy*, 3(1), 7–14. DOI: 10.1515/cse-2016-0003
- [3] Kurbanova, D.G., Teshabayev, Z.A., Nasulayev, H.A., Gulomov, Sh.T., Boymonov, R.M., Turdieva, D.P., Rakhimjonov, B.B. (2020). Processing of spent adsorbents and catalysts into protective layers for oil and gas processing. *Vestniknauz, kimyo*, 3(1), 263–266.
- [4] Hongjun, Z., Mingliang, S., Huixin, W., Zeji, L., Hongbo, J. (2010). Modeling and simulation of moving bed reactor for catalytic naphtha reforming. *Petroleum Science and Technology*, 28, 667–676. DOI: 10.1080/10916460902804598
- [5] Kiryanov, D.I., Smolikov, M.D., Golinsky, D.V., Belopukhov, E.A., Zatulokina, E.V., Udras, I.E., White, A.S. (2018). History of development and current status of the catalytic reforming process in Russia. Experience of industrial production and operation of new reforming catalysts series PR. *Rossiiskii Khimicheskii Zhurnal (Russian Chemistry Journal)*, 62(1–2), 12–23. DOI: 10.6060/rcj.2018621-2.2
- [6] Rahimpour, M.R., Jafari, M., Iranshahi, D. (2013). Progress in catalytic naphtha reforming process: A review. *Applied Energy*, 109, 79–93. DOI: 10.1016/j.apenergy.2013.03.080
- [7] Chernyakova, E.S., Koksharov, A.G., Ivanchina, E.D., Yakupova, I.V. (2015). Heavy naphtha fractions 85-155°C recycling in the catalytic reforming industrial unit. *Procedia Chemistry*, 15, 378–383. DOI: 10.1016/j.proche.2015.10.060
- [8] Rodríguez, M.A., Ancheyta, J. (2011). Detailed description of kinetic and reactor modeling for naphtha catalytic reforming. *Fuel*, 90, 3492–3508. DOI: 10.1016/j.fuel.2011.05.022
- [9] Mazzieri, V.A., Grau, J.M., Vera, C.R., Yori, J.C., Parera, J.M., Pieck, C.L. (2005). Role of Sn in Pt-Re-Sn/Al₂O₃-Cl catalysts for naphtha reforming. *Catalysis Today*, 107–108, 643–650. DOI: 10.1016/j.cattod.2005.07.042
- [10] Viswanadham, N.N., Kamble, R., Sharma, A., Kumar, M., Saxena, A.K. (2008). Effect of Re on product yields and deactivation patterns of naphtha reforming catalyst. *Journal of Molecular Catalysis A: Chemical*, 282, 74–79. DOI: 10.1016/j.molcata.2007.11.025
- [11] Smolikov, M.D., Kiryanov, D.I., Kolmagorov, K.V., Udras, I.E., Zatulokina, E.V., White, A.S. (2013). Experience of industrial production and operation of new reforming catalysts PR-81 and ShPR-81. *Catalysis in Industry*, 6, 36–41. DOI: 10.1134/S2070050414010115
- [12] Gurdin, V.I., Kovalenko, M.V., Krasiy, B.V., Mozhaiko, V.N., Sorokin, I.I. (2016). Highly stable reforming catalyst series RB in ball form. *Refining and Petrochemicals*, 10, 11–14.

- [13] Baghalha, M., Mohammadi, M., Ghorbanpour, A. (2010). Coke deposition mechanism on the pores of a commercial Pt–Re/c-Al₂O₃ naphtha reforming catalyst. *Fuel Processing Technology*, 91, 714–722. DOI: 10.1016/j.fuproc.2010.02.002
- [14] Ostrovskii, N.M. (2006). General equation for linear mechanisms of catalyst deactivation. *Chemical Engineering Journal*, 120, 73–82. DOI: 10.1016/j.cej.2006.03.026
- [15] Stijepovic, M.Z., Linke, P., Kijevcanin, M. (2010). Optimization approach for continuous catalytic regenerative reformer processes. *Energy Fuels*, 24, 1908–1916. DOI: 10.1021/ef901193v
- [16] Patent RU 2171710 B01 J 20/08, B01 J 20/04, published 10.08.2001
- [17] Patent RU 2662540 C2 B01D 53/68, B01 J 20/02, published 26.07.2018
- [18] Patent RU 2219995 C2 B01 J 20/08, B01 J 53/68, 27.12.2003
- [19] Shah, I.K., Pre, P., Alappat, B.J. (2013). Steam Regeneration of Adsorbents: An Experimental and Technical Review. *Chemical Science Transactions*, 2(4), 1078–1088. DOI: 10.7598/cst2013.545
- [20] Solodova, N.L., Cherkasova, E.I., Salakhov, I.I., Tutubalina, V.P. (2017). Hydrogen as an energy carrier and reagent. Technologies of its production. *Problems of Power Engineering*, 19, 11–12.
- [21] Schaedel, B.T., Duisberg, M., Deutschmann, O. (2009). Steam reforming of methane, ethane, propane, butane, and natural Gas over a rhodium based catalyst. *Catalysis Today*, 142, 42–51. DOI: 10.1016/j.cattod.2009.01.008
- [22] Fernandez, J.R., Abanades, J.C., Murillo, M. (2012). Modeling of sorption enhanced steam Methane reforming in an adiabatic fixed bed reactor. *Chemical Engineering Science*, 84, 1–11. DOI: 10.1016/j.jece.2021.105863
- [23] Astanovskiy, D.L., Astanovskiy, L.Z., Kustov, P.V. (2016). Energy-saving, environmentally friendly production of hydrogen from hydrocarbon raw materials. *Neftegazokhimiya*, 3, 10–16.
- [24] Maestry, M., Vlachos, D.G., Beretta, A., Gropi, G., Tronconi, E. (2008). Steam and dry reforming of methane on Rh: Microkinetic analysis and hierarchy of kinetic models. *Journal of Catalysis*, 259, 211–222. DOI: 10.1016/j.jcat.2008.08.008
- [25] Pisarenko, E.V., Pisarenko, V.N. (2001). Energy- and resource-saving process of synthesis gas production from natural gas in methanol production. *Theoretical Fundamentals of Chemical Technologies*, 45(4), 371.
- [26] Kuznetsov, V.V., Vitovsky, O.V., Gasenko, O.A. (2009). Methane steam reforming in an annular microchannel with Rh/Al₂O₃ catalyst. *Journal of Engineering Thermophysics*, 18, 187–196. DOI: 10.1134/S1810232809030023
- [27] Peighambardoust, S.J., Rowshanzamir, S., Amjadi, M. (2010). Review of the proton exchange membranes for fuel cell applications. *International Journal of Hydrogen Energy*, 35(17), 9349–9384. DOI: 10.1016/j.ijhydene.2010.05.017
- [28] Snytnikov, P.V., Badmaev, S.D., Volkova, G.G., Potemkin, D.I., Zyryanova, M.M., Belyaev, V.D., Sobyanin, V.A. (2012). Catalysts for hydrogen production in a multifuel processor by methanol, dimethyl ether and bioethanol steam reforming for fuel cell applications. *International Journal of Hydrogen Energy*, 37(21), 16388–16396. DOI: 10.1016/j.ijhydene.2012.02.116
- [29] Zyryanova, M., Badmaev, S.D., Belyaev, V.D., Amosov, Y.I., Snytnikov, P.V., Kirillov, V.A., Sobyanin, V.A. (2013). Catalytic conversion of hydrocarbon raw materials into fuel for power plants. *Catalysis in Industry*, 3, 22–27. DOI: 10.1134/S2070050413040107
- [30] Molodozhenyuk, T.B., Vorobyov, V.N., Ishanova, L.R., Razikov, K.Kh. (1984). Study of destructive-epitaxial and thermal transformations in the MgO–Al₂O₃–H₂O system. *Journal of Applied Chemistry*, 7, 1454–1459.
- [31] Mustafayev, B.D., Turdiyeva, D.P., Kurbanova, D.G., Rakhimjonov, B.B., Isayeva, N.F., Satarova, Sh.G. (2020). Effect of aluminum oxide precursor on the formation of sodium aluminates in the adsorbent composition. *Ilm-fan va Innovatsion Rivozhlanish*, 5, 124–134.
- [32] Ledovskaya, E.G., Gabelkov, S.V., Litvinenko, L.M., Logvinkov, D.S., Mironova, A.G., Odeichuk, M.A., Poltavtsev, N.S., Tarasov, R.V. (2006). Low temperature synthesis of magnesium-aluminum spinel. *Voprosy Atomnoj Nauki i Tekhniki*, 1, 160–163.
- [33] Domanski, D., Urretavizcaya, G., Castro, F.J., Gennari, F.C. (2004). Mechanochemical synthesis of magnesium aluminate spinel powder at room temperature. *Journal of the American Ceramic Society*, 87(11), 2020–2024. DOI: 10.1111/j.1151-2916.2004.tb06354.x
- [34] Ishimaru, M., Hirotsu, Y., Afanasyev-Charkin, I.V., Sickafus, K.E. (2002). Atomistic structures of metastable and amorphous phases in ion-irradiated magnesium aluminate spinel. *Journal of Physics: Condensed Matter*, 14(6), 1237–1247. DOI: 10.1088/0953-8984/14/6/311

- [35] Senina M.O., Lemeshev, D.O. (2016). Ways of synthesizing powders of magnesium aluminate spinel for obtaining optically transparent ceramics (review). *Advances in Chemistry and Chemical Technology*, 7, 101–103. DOI: 10.1007/s10717-018-9994-8
- [36] Ganesh, J.A. (2013). Review on magnesium aluminate ($MgAl_2O_4$) spinel: synthesis, processing and applications. *International Materials Reviews*, 115(16), 63–112. DOI: 10.1179/1743280412Y.0000000001
- [37] Yunusov, M.P., Saidaxmedov, Sh.M., Djalalova, Sh.B., Nasullaev, Kh.A., Gulyamov, Sh.T., Isaeva, N.F., Mirzaeva, E.I. (2015). Synthesis and Study of Ni-Mo-Co Catalysts for Hydroprocessing of Oil Fractions. *Catalysis for Sustainable Energy*, 2(1), 43–56. DOI: 10.1515/cse-2015-0003
- [38] Isayeva, N.F., Jalalova, Sh.B. (2012). Technology of preparation of carriers on the basis of aluminum hydroxide of different shelf life, *Uzbek Journal of Oil and Gas*, 1, 27–31.